Field Demonstration of a Battery-Free Decentralized Solar-Hydrogen Clean Cooking

Runjhun Shah [a], Arun S Raj[b], Ronita Bardhan[c], Prakash C Ghosh [a*]

[a] Department of Energy Science and Engineering
Indian Institute of Technology Bombay
Powai, Mumbai-400076, India

[b] Zest Clean Power Private Limited,
Saki Vihar Road, Chandivali, Mumbai-400072, India

[c] Sustainable Built Environment and Health,
University of Cambridge
Cambridge, United Kingdom

*Corresponding Author:
Prof. Prakash C. Ghosh
Department of Energy Science and Engineering
Indian Institute of Technology Bombay
Powai, Mumbai 400076, Maharashtra, India
E-mail: pcghosh@iitb.ac.in
Tel.: +91-22-2576-7896

Field Demonstration of a Battery-Free Solar-to-Hydrogen Decentralized Solution for Clean Cooking

Runjhun Shah [a], Arun S Raj[b], Ronita Bardhan[c], Prakash C Ghosh [a*]

[a] Department of Energy Science and Engineering, Indian Institute of Technology Bombay, Powai, Mumbai-400076, India
[b] Zest Clean Power Private Limited, Powai, Mumbai-400076, India
[c] Sustainable Built Environment and Health, University of Cambridge, Cambridge, United Kingdom

Abstract

Clean cooking remains a major energy-access challenge, particularly where cooking fuels depend on centralized supply chains. This study demonstrates a battery-free solar-to-hydrogen cooking system comprising a 1.74 kWp photovoltaic array, 1 kW alkaline electrolyser, hydrogen storage and a pure-hydrogen burner. The system was coupled through a maximum power point tracking controller and operated from November 2024. Detailed characterization on 16 December 2024 produced 7.5 kWh of solar electricity and approximately 1.3 m^3 of hydrogen, equivalent to 3.9 kWh on a lower-heating-value basis. Hydrogen production reached approximately 3 L min^{-1}, while burner efficiency ranged from 35% to 46%. At 9.7 L min^{-1}, 1 L of water reached boiling in 6.2 min compared with 5.0 min for LPG. The local temperature rise was approximately 2 °C for hydrogen versus 9 °C for LPG. The results demonstrate the technical feasibility of decentralized solar-to-hydrogen cooking under field conditions.

Keywords:

Clean cooking; green hydrogen; energy storage; decentralized energy systems; alkaline electrolyser; solar photovoltaics

1. Introduction

Access to clean cooking remains a persistent challenge in the transition toward sustainable and equitable energy systems. Despite improvements in access to modern fuels, approximately two billion people continued to rely primarily on polluting cooking fuels and technologies in 2024 [1,2]. The associated burden of household air pollution, together with fuel affordability, supply reliability and distribution constraints, motivates the investigation of decentralized clean-cooking pathways [2,3,4,5]. In India, liquefied petroleum gas (LPG) has supported the transition away from traditional solid fuels, but reliance on delivered fuels presents continuing concerns regarding affordability and energy security [4,5]. These considerations create a need to evaluate locally produced renewable cooking energy, while distinguishing technical feasibility from the economic and social conditions required for widespread adoption.

Solar photovoltaic (PV) technologies offer a modular route to renewable cooking energy, either through direct electric cooking or conversion to other energy carriers. Studies of PV-based cooking and PV microgrids demonstrate the potential to couple renewable electricity supply with cooking loads [6-8]. Opoku et al. developed a 150 Wp pressurized solar electric cooker using erythritol phase-change storage and reported successful rice cooking [9]. More recently, Chaciga et al. experimentally investigated an indoor PV cooker with thermal-oil and rock-pebble storage, reporting approximately 9 kWh of storage capacity and cooking during charging and discharge [10]. Nyeinga et al. subsequently examined the design and cooking characteristics of a PV-powered heating-funnel configuration for institutional use [11]. A systematic review by Odoi-Yorke et al. identifies improved device design, energy-storage integration, economic assessment and alternative energy carriers among priorities for solar PV cooking research [12]. A PV mini-grid case study in a refugee settlement likewise found that efficient electric pressure cooking can be integrated into an optimized electricity supply system, although investment and operational conditions remain important [13]. These results support direct electrification as a practical reference pathway against which alternative storage architectures should be evaluated.

The intermittency of PV generation nevertheless complicates matching cooking demand to renewable energy availability [14]. Batteries and sensible- or latent-heat storage can improve this match, but introduce additional equipment, losses, cost or application-specific operating constraints. Renewable hydrogen provides a distinct means of storing solar electricity as a chemical fuel: electricity from a PV array drives water electrolysis, the resulting hydrogen is stored, and the fuel can subsequently be converted directly into cooking heat. This does not establish a universal advantage over direct PV-powered cooking, since electrolysis and subsequent combustion add conversion losses. Rather, hydrogen may be complementary where the availability of a storable gaseous fuel, temporal flexibility or the desire to avoid electrochemical battery storage motivates evaluation of another energy pathway [15-17]. Recent analyses emphasize that green hydrogen is most appropriately considered alongside, rather than automatically in place of, technically feasible direct electrification [18].

Renewable hydrogen has been examined extensively for residential and decentralized power applications. Özçelep et al. investigated a PV–hydrogen system for household energy demand and hydrogen blending with natural gas [19], while Gil Mena et al. compared stand-alone solar–battery and solar–hydrogen configurations for collective residential energy supply [20]. Khan et al. analysed a hydrogen-based hybrid system for reliable rural electricity supply [21], and Çiçek considered hydrogen storage, a fuel cell, electrolyser and household end uses, including a hydrogen hob, in a resilience-oriented energy management model [22]. PV–electrolyser system studies also demonstrate that component sizing, operating strategy and renewable-electricity variability materially affect hydrogen production and economic outcomes [23-25]. These contributions establish the relevance of integrated renewable-hydrogen systems but do not, in themselves, provide field evidence for the complete PV-to-hydrogen-to-cooking pathway considered here. Moreover, using hydrogen as a storage medium for fuel-cell-based electric cooking suffers from low efficiency and high capital costs.

Hydrogen has also been studied directly as a cooking fuel. Fumey et al. developed a hydrogen stove based on catalytic oxidation over platinum-coated porous silicon-carbide ceramics, obtaining cooking efficiencies of up to 80% under their test protocol [26]. Their work establishes the technical potential of direct conversion of stored hydrogen into cooking heat, while illustrating the importance of burner configuration and heat-transfer design. However, key challenges include a short burner lifespan caused by thermal cycling and high material costs due to the platinum catalyst. Topriska et al. combined experimental results and numerical analysis for solar-hydrogen cooking applications [27], and subsequent studies explored possible hydrogen-cooking applications in different geographic settings [28]. Mukelabai et al. reviewed hydrogen cooking technologies, renewable hydrogen supply systems and techno-economic issues [16]; Zhao et al. assessed technical and economic feasibility and deployment barriers in developing countries [17]; Hutty et al. considered integrated lead-acid battery–electrolyser configurations for cooking [29]; and Odoi-Yorke et al. evaluated the economics of decentralized PV-based hydrogen cooking in Ghana [30]. Together, this work demonstrates substantial progress, although studies vary considerably in component arrangement, operating scale, and whether results are based on modelling or experimental measurements.

In addition to efficiency and energy supply, household hydrogen cooking requires attention to burner safety, flame visibility and user interaction. Scott and Powells found that prospective users considered hydrogen flame characteristics particularly consequential for cooking practices [31]. Gordon et al. showed that attitudes toward domestic hydrogen involve environmental engagement, familiarity and differences across users [32], while a related study identified safety and perceived appliance performance as determinants of potential residential hydrogen adoption [33]. These studies do not evaluate the present burner, but they underscore why field-level burner observations and clearly bounded claims are important.

An important remaining research need is therefore the integrated experimental evaluation of a decentralized solar-to-hydrogen cooking system in which variable PV generation drives an electrolyser without intermediate battery storage, hydrogen is retained as the energy-storage medium, and a hydrogen-compatible burner supplies the cooking heat. Existing component, appliance and techno-economic studies offer essential foundations, but evidence connecting solar generation, PV–electrolyser electrical matching, hydrogen generation and storage, and end-use burner performance under actual outdoor operating conditions remains comparatively limited. In an MPPT-mediated arrangement, the PV array and electrolyser are electrically coupled through power electronics rather than being directly connected at their terminals; this distinction matters when interpreting conversion and control losses [23,24].

To address this need, the present study presents a field demonstration of a battery-free solar-to-hydrogen cooking system comprising a 1.74 kWp PV array, a 1 kW alkaline electrolyser, hydrogen storage and a post-mixed pure-hydrogen burner. The proposed porous metallic burner produces a visible orange hydrogen flame, enhancing safety and cultural acceptance compared to radiative burners. Featuring a ~5 μm pore size that inherently prevents flashback across all flow rates, this catalyst-free and thermal-cycling-resistant metallic design provides a cost-effective, durable, and sustainable cooking solution. The PV array supplies the electrolyser through a maximum power point tracking (MPPT) controller, with no electrochemical battery in the energy chain. Operation began in November 2024, and detailed characterization was carried out on 16 December 2024 under clear-sky conditions. The investigation quantifies daily PV electricity generation, electrolyser operation and hydrogen production; evaluates the hydrogen burner's water-heating performance at different fuel flow rates; and compares boiling behaviour and local cooking-area temperature rise with an LPG burner. The contribution is an integrated field-scale assessment of the solar-electricity-to-stored-hydrogen-to-cooking-heat pathway, together with identification of constraints that must be addressed before conclusions can be drawn regarding long-term reliability, safety, economic competitiveness or broad household adoption.

2. Materials and Methods

2.1. System Architecture

The experimental system comprises a solar photovoltaic (PV) array, a maximum power point tracking (MPPT) controller, an alkaline electrolyser, a hydrogen storage system, and a pure hydrogen-compatible cooking burner. A schematic representation of the integrated solar–hydrogen cooking system, illustrating the energy flow (Fig 1a).

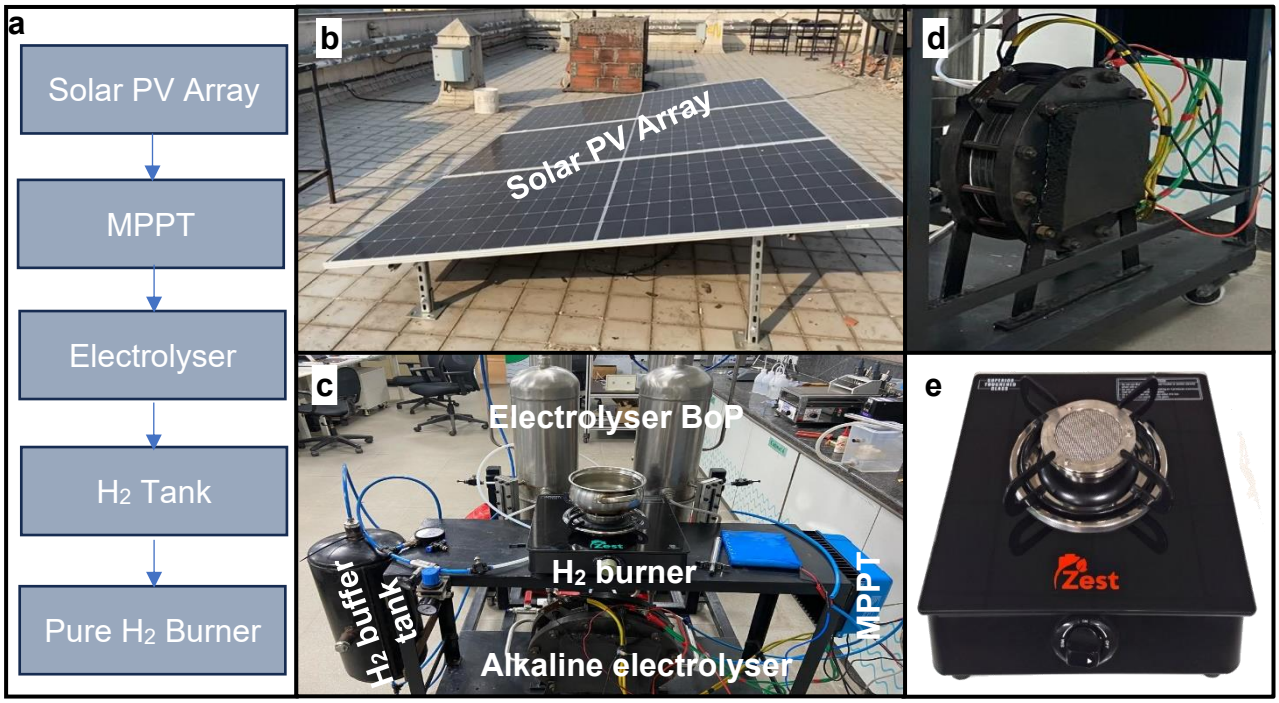


Fig. 1. Experimental setup of the solar hydrogen cooking system. (a) Schematic illustration of the energy flow from the photovoltaic (PV) array to the hydrogen cooking stove, including hydrogen production and storage. **(b)** Photograph of the solar PV array used in the study. **(c)** Photograph of the integrated hydrogen generation, storage and cooking system. **(d)** Photograph of the 1 kW alkaline electrolyser employed for hydrogen production. **(e)** Photograph of the pure hydrogen cooking burner used in the experiments.

The system was intentionally designed without battery storage in order to reduce the overall operational cost associated with energy storage. Instead, the solar PV array is directly coupled to the electrolyser through the MPPT controller, producing hydrogen in real-time during periods of solar availability. The MPPT unit used for this purpose is the SmartSolar MPPT 250/100-Tr VE from Victron Energy, which facilitates efficient power transfer between the solar PV array and the electrolyser.

2.1.1. Solar Photovoltaic System

The system consists of three solar photovoltaic (PV) panels, each with a capacity of 580 Wp, connected in series. These panels are installed on the terrace of the Department of Energy Science and Engineering, IIT Bombay (Fig. 1b).

The solar PV array is directly connected to the alkaline electrolyser through an MPPT controller with a capacity of 1450 W when operated at 12 V. Based on the power available from the solar array at the MPPT input (Fig. 1c), the controller dynamically adjusts its output to match the operating characteristics of the alkaline electrolyser, ensuring efficient energy transfer. The

specifications of the solar PV panels and the MPPT controller used in the present study are summarized in Table 1.

2.1.2. Alkaline Electrolyser System

The system comprises an indigenously developed alkaline electrolyser stack consisting of five cells connected in series with a capacity of approximately 1 kW when operated at 12 volts, designed for small-scale hydrogen production (Fig. 1d). Each cell has an active area of approximately 176 cm^2. A Zirfon® separator with a thickness of 500 µm is employed in the electrolyser, while nickel-based electrodes are used for both the anode and cathode. A 30 wt% KOH solution is used as the electrolyte. The electrolyser is designed to operate at a pressure of up to 15 bar.

2.1.3. Hydrogen Storage Tank

A commercially available Type-I hydrogen storage tank with a water capacity of 47 L is used for hydrogen storage and is directly coupled to the outlet of the alkaline electrolyser. The storage tank can accommodate approximately 63g of hydrogen, which corresponds to nearly 2 kWh of chemical energy based on the lower heating value (LHV). For context, the average useful household cooking-energy requirement in India has been estimated at approximately 7 MJ/day (1.94 kWh/day) after accounting for stove efficiencies [34]. Because hydrogen can also be consumed directly as it is produced during periods of solar availability, the storage tank provides additional flexibility for cooking outside periods of active hydrogen production.

2.1.4. Pure Hydrogen Burner

An indigenously developed post-mixed porous burner by Zest Clean Power Pvt. Ltd. is employed for combustion of pure hydrogen (Fig. 1e). The proposed porous metallic burner, with a pore size of ~5 µm, combusts pure hydrogen with a visible orange flame. This addresses safety concerns surrounding invisible hydrogen flames and satisfies cultural preferences for flame-based cooking, enhancing user adoption relative to radiative burners. Furthermore, because the design operates without precious-metal catalysts, it offers a cost-effective solution, while its fine pore structure inherently prevents flashback across all hydrogen flow rates. Furthermore, because the metallic porous bed is not subject to severe thermal cycling, it is expected to deliver a long operational lifespan. This durability, in turn, provides a highly cost-effective and sustainable solution for hydrogen-based cooking. A full safety-code assessment for unattended household deployment, covering ventilation requirements, leak-detection provisions, and applicable domestic gas-appliance standards, was outside the scope of this study and is identified as necessary work before wider dissemination.

2.2. Hydrogen Production Estimation

The system has been operating since 2024, during which the electrolyser was powered by solar-generated electricity regulated through a Maximum Power Point Tracking (MPPT) controller. System data was monitored and recorded using the Cerbo GX unit from Victron Energy. A detailed performance analysis of the system was carried out for the entire month of December 2024.

Hydrogen production is estimated using operating current of the electrolyser derived from MPPT output current. The hydrogen yield in LPM is estimated using equation given below.

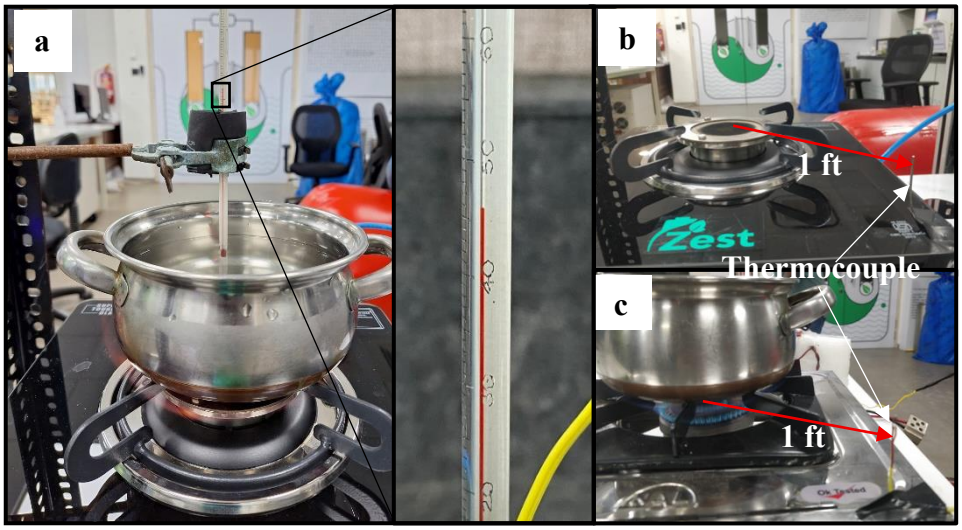


Fig. 2. Experimental setup for evaluating hydrogen burner performance. (a) Cooking efficiency using the water-boiling method. (b) Assessment heat stress induced by a hydrogen flame. (c) Assessment heat stress induced by an LPG flame

$$\dot{m_{H_2}} = \left(\frac{\dot{\iota_{MPPT}} - \iota_{leakage}}{n \cdot F}\right) \cdot \left(\frac{m_{H_2}}{\rho_{H_2}}\right) \cdot n_{cell} \cdot 60 \quad (1)$$

where,

i_{MPPT}: Current from MPPT to electrolyser in ampere

n_{cell} : Number of cells in a stack

m_{H_2}: Molecular weight of hydrogen in gram

ρ_{H_2}: Density of hydrogen in gram per litre

F: Faraday's constant

n: No of electrons released per mole of hydrogen

$i_{leakage}$: leakage current in the electrolyser which does not contribute to the electrochemical conversion and leads to a direct ohmic loss and can be given

$$i_{leakage} = i_{leakage_ref} \cdot \frac{V_{op}}{V_{ref}} \quad (2)$$

where, $i_{leakage_ref}$ refers to a current through the electrolyser stack when the operating voltage is maintained at V_{ref} and V_{op} is actual operating voltage of the stack.

Corresponding water consumption in millilitre per minute estimated using equation given below.

$$\dot{m_{H_2O}} = \left(\frac{\dot{\iota_{MPPT}} - \iota_{leakage}}{n \cdot F}\right) \cdot 0.018 \cdot n_{cell} \cdot 60 \quad (3)$$

2.3. Hydrogen Burner Testing

The performance of the hydrogen burner is evaluated and compared with a conventional LPG burner having a power rating of 2 kW. The burner efficiency was determined by heating one litre of water from ambient temperature to its boiling point (Fig. 2a). The vessel is made of stainless steel with a total mass of 347g.

To assess the performance of the burner, the fuel flow rate was varied, and the corresponding variation in water temperature with time was recorded. Based on these measurements, the burner efficiency was estimated using the following equation:

$$\eta_{burner} = \frac{m \cdot C_p \cdot \Delta T}{\dot{m}_{H_2} \cdot \rho_{H_2} \cdot \Delta H_{LHV} \cdot \Delta t} \quad (4)$$

where,

m: Mass of water (kg)
C_p: Specific of water (J kg^{-1} ^{o}C^{-1})
ΔT: Rise of temperature (^{o}C)
$\dot{m}_{H_2}$: Flow rate of hydrogen (L s^{-1})
ΔH_{LHV}: Lower heating value (J mol^{-1})
ρ_{H_2}: Molar density of hydrogen (mol L^{-1})
Δt: Time (s)

To quantify the heat stress associated with hydrogen (Fig. 2b) and LPG flames (Fig. 2c), thermocouples were placed at a distance of 1 ft from the center of each burner. The temperature rise at steady state was measured and compared to assess the heat exposure experienced by a person positioned near hydrogen and LPG flames.

3. Results

3.1. Solar Power Generation

The specifications of the different components are summarized in Table 1. Although the proposed system has been operational since November 2024, demonstrating sustained day-to-day functioning over this period, a detailed performance study was carried out in December 2024 to evaluate the feasibility of hydrogen as a cooking medium and to assess the system's behaviour over a full day. A representative clear day (16 December 2024) was selected so that full-day performance could be characterised under favourable and reproducible conditions.

Table 1: Summary of different components used in the system.

Photovoltaic panel electrical parameters at STC (Irradiance: 1000 W m^{-2}, Temp.: 25 ^{o}C, Air Mass: 1.5)	
Peak power (kWp)	0.580
Open circuit potential (V)	51.48
Short circuit current (A)	14.36
Potential at maximum power (V)	43.22
Current at maximum power (A)	13.42
Fill factor (%)	79
MPPT details	
Rated current (A)	100
Operating voltage (V)	12/24/48
Maximum power (W)	1450/2900/5800
Electrolyser stack details	
Number of cells	5
Active area (cm^2)	176
Operating voltage (V)	12
Current at operating voltage (A)	100
Operating pressure (bar)	15
Separator thickness (μm)	500
KOH concentration (wt%)	30

Hydrogen storage details	
Type of tank	Type I
Rated maximum pressure (bar)	150
Maximum operating pressure (bar)	15
Mass of H_2 at max. op. pressure (gm)	63
Total energy storage capacity (kWh)	2
Water Volume (L)	47
Hydrogen burner details	
Rated power (kW)	1.8
Rated flow rate (LPM)	10
Maximum flow rate (LPM)	12
Rated inlet pressure (mbar)	20
Minimum operating power (W)	90
Minimum operating flow rate (LPM)	0.5

The current–voltage characteristics of the system over the course of the day (Fig. 3) show a peak voltage of 137 V and a peak current of 10 A. It is observed that the power output drops sharply after 15:00 hours due to shading caused by a high-rise building located to the southwest of the PV array. As a result, only diffuse solar radiation is available during this period, leading to a significant reduction in power generation.

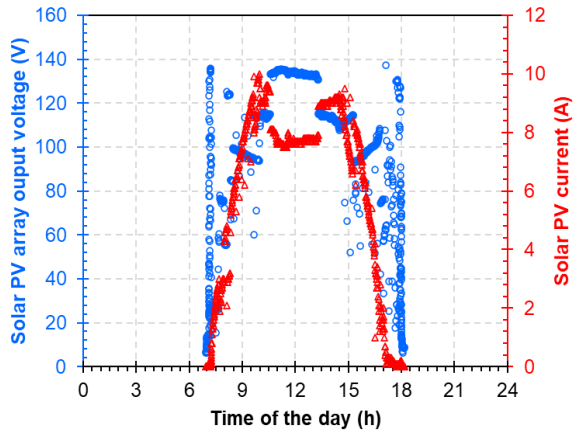


Fig. 3. Diurnal current voltage profile of the solar-powered hydrogen cooking system for single-household applications

The instantaneous power output and cumulative energy generation of the photovoltaic array over the course of the day (Fig. 4.) indicate a total daily energy generation of 7.5 kWh. Considering the installed capacity of 1.74 kWp, the system achieved a daily yield of 4.3 kWh/kWp. The observed instantaneous peak power is found to be only 1.1 kW as the current was restricted by the MPPT to 90 A.

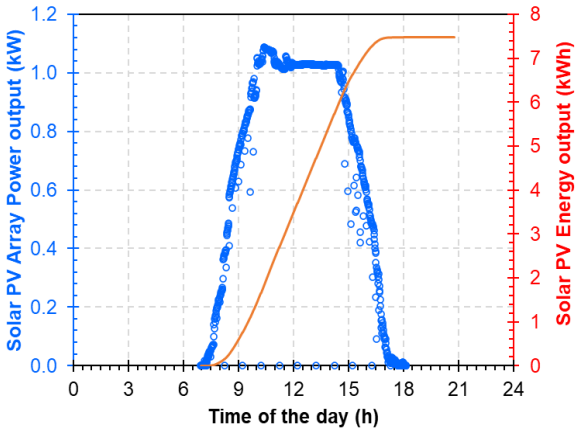


Fig. 4. Instantaneous MPPT power output and cumulative energy input to the alkaline electrolyser

3.2. Alkaline electrolyser performance

The current–voltage characteristics of the electrolyser (Fig. 5) show a progressive decrease in the operating voltage with increasing operating temperature, indicating improved electrolyser performance. As the power output of the PV array increases with time, a corresponding rise in both current and voltage are observed. Notably, the I–V characteristics exhibit a hysteresis behavior, which can be attributed to variations in the operating temperature of the electrolyser.

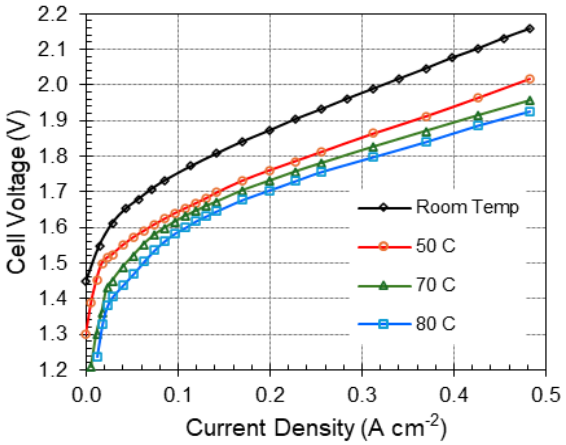


Fig. 5. Polarization behaviour of the alkaline electrolyser stack.

The current and voltage profiles of the alkaline electrolyser throughout the day correspond to the output of the maximum power point tracker (MPPT), as the electrolyser is directly coupled to the MPPT (Fig. 6). Although the rated current of the electrolyser is 100 A, the maximum operating current was limited to 90 A. This operational constraint reduced the daily energy yield of the system, as the solar PV array was forced to operate at lower power levels between 10:00 hours and 14:20 hours.

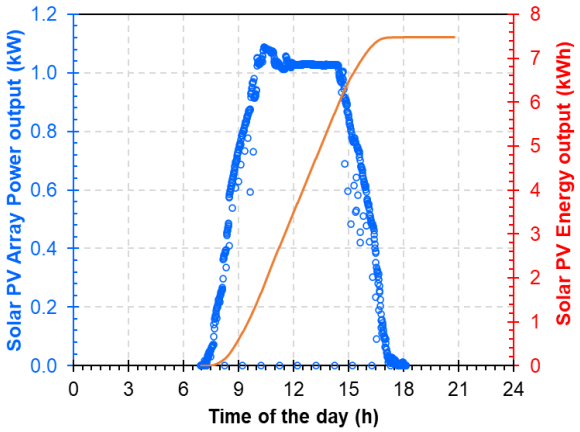


Fig. 6. Current and voltage profiles of the electrolyser during operation.

In the morning, the electrolyser operates near ambient temperature. As the day progresses, the temperature gradually increases, reaching a maximum of approximately 70°C around 14:20 hours. The operating potential of the electrolyser stack was found to be from 11.48 V at 10:00 hours, which drops to 11.18 V at 14:20 hours (Fig. 7). In the afternoon, beyond this point, the elevated operating temperature enhances the conversion efficiency of the electrolyser, resulting in a reduction in the operating voltage for a given current. This temperature-dependent behavior leads to the observed hysteresis in the electrolyser characteristics.

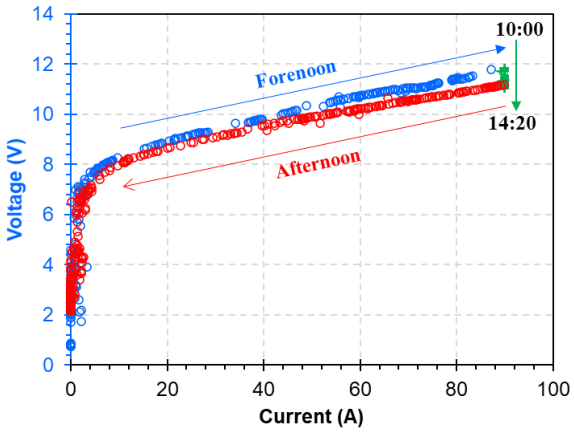


Fig.7. Electrolyser polarization characteristics derived from the measured current–voltage data during operation.

The hydrogen production rate of the electrolyser was quantified using equations (1) and (2) (Fig. 8). During peak solar insolation hours, the electrolyser operated at a rated power of 1 kW, achieving a peak hydrogen generation rate of approximately 3 LPM. The cumulative hydrogen production on the day of study was about 1.3 m^3 (at standard conditions), which corresponds to an energy-equivalent volume of approximately 0.46 m^3 of piped natural gas (PNG).

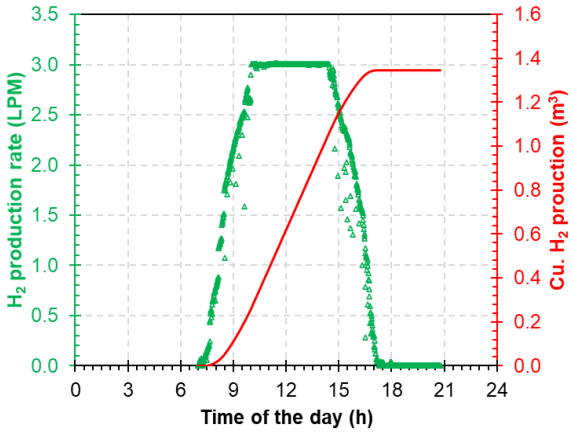


Fig. 8. Instantaneous hydrogen production rate and cumulative daily hydrogen generation.

The temporal variation of water consumption in the electrolyser estimated using equation (3) is presented in Extended Data Fig. 1. The total water consumption recorded over the study period was approximately 1.1 Litre. This observed consumption is consistent with the stoichiometric requirement of water for electrolysis, with minor deviations attributable to system inefficiencies and ancillary losses.

3.3. Pure Hydrogen Burner Performance

The hydrogen flow rate was varied from 1 to 10 LPM, and the corresponding flame characteristics were examined. The hydrogen flame exhibited a yellowish-red appearance under the tested conditions. As the hydrogen flow rate increased, the flame height was observed to increase progressively, (Fig. 9(a–f)). The pressure drop in the hydrogen stove primarily arises from two components: the burner and the flow-regulating device integrated into the system.

The variation of total pressure drop with hydrogen flow rate shows that the burner contributes a relatively minor pressure drop, approximately 3 mbar at a hydrogen flow rate of 10 LPM (Fig. 9g). In contrast, the regulator accounts for a significantly larger pressure drop of about 20 mbar under the same operating condition. Consequently, the combined pressure drops across the stove assembly reaches approximately 23 mbar at a hydrogen flow rate of 10 LPM.

These results indicate that the regulator constitutes the dominant flow resistance within the system, thereby playing a critical role in determining the overall pressure requirements and flow stability of the hydrogen supply to the burner.

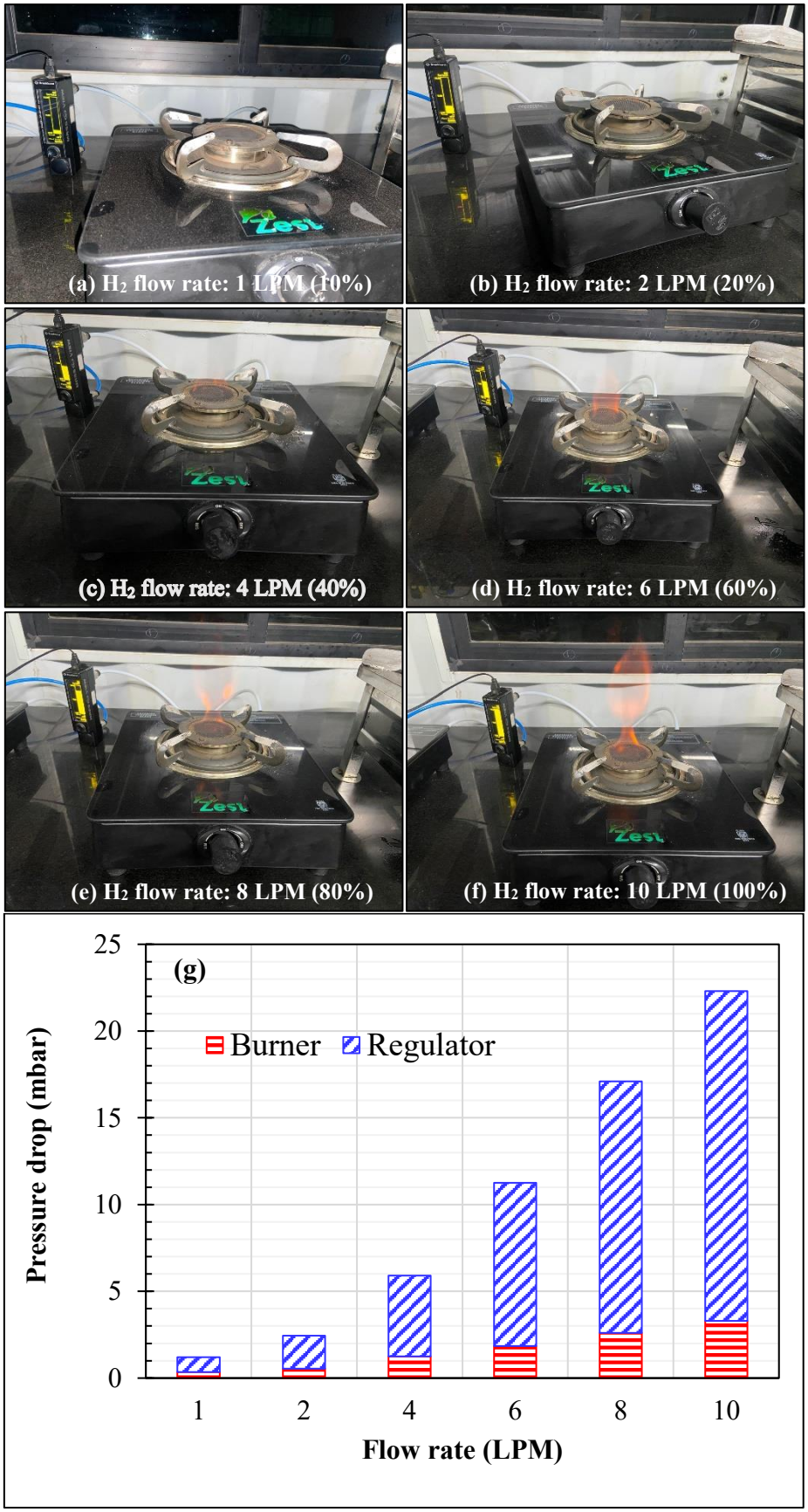


Fig. 9. Performance of the pure hydrogen burner at different hydrogen flow rates. **(**a)–(f) Flame images at hydrogen flow rates of 1, 2, 4, 6, 8 and 10 L min^{-1}**,** respectively, **(g)** Corresponding pressure drop across the hydrogen burner and pressure regulator as a function of hydrogen flow rate.

3.4. Comparison between LPG and Hydrogen burner

Experimental results comparing hydrogen burner operation with standard LPG burner conditions are presented, focusing on hydrogen flow rates, flame characteristics, and the ability to achieve equivalent cooking performance (Fig.10).

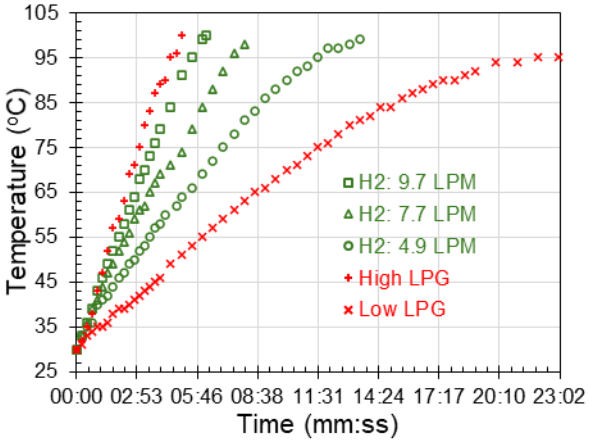


Fig. 10. Comparison of the thermal performance of pure hydrogen and LPG burners through water boiling time as a function of fuel flow rate

For comparing the time variation in cooking between hydrogen burner and LPG burner, a standard testing protocol was adopted. One litre of water at 30 °C is heated to 100 °C using both hydrogen burner and the LPG burner at varied flow rates. The hydrogen burner was operated at 9.7, 7.7 and 4.9 LPM and compared with a conventional LPG burner at its high and low flame settings. The LPG high setting brought the water to boiling (100 °C) in 5.0 minutes, while the hydrogen burner at 9.7 LPM reached 100 °C in 6.2 min, showing that the hydrogen burner achieves a heating rate close to that of LPG at full flame. The heating slowed as the hydrogen flow rate was reduced, the water reaching 98 °C in 8.0 min at 7.7 LPM and 99 °C in 13.0 min at 4.9 LPM. Using the water-boiling method, the thermal efficiency of the hydrogen burner was found to increase with flow rate, from 34.5% at 4.9 LPM to 38.6% at 7.7 LPM and 46.0% at 9.7 LPM. By contrast, the LPG low setting did not bring the water to a boil, attaining only about 95°C after 23 min of heating. This is likely because, at low flame settings, heat losses through evaporation and convection from the vessel walls approach the rate of heat supplied by the flame, so the water temperature equilibrates below boiling point. All three flow rates considered for hydrogen are beyond this minimum threshold, and the burner performance at high flow rate of 9.7 LPM is comparable to that of the high setting of LPG burner. In fact, for the first twenty-degree rise, the performance of both these burners at the highest setting are practically identical showing comparable operation.

3.5. Heat stress

The heat stress from hydrogen and LPG flames was compared by measuring the temperature rise at a fixed distance from the burner. The hydrogen flow rate was maintained at 10 LPM, assuming that the total thermal power is comparable to that of an LPG flame when the regulator is set to a high position. The ambient air temperature surrounding the burner was measured at a radial distance of 1 ft to quantify the thermal environment experienced by the user is presented in Fig. 11. Under the LPG flame the temperature rose progressively over the first ~4 minutes and then levelled off at approximately 9°C, whereas under the hydrogen flame it remained close to 1°C for almost the entire period, rising to about 2°C only towards the end. The steady-state temperature

rise near the cook was therefore reduced from approximately 9°C with LPG to about 2°C with hydrogen, a reduction of about 7°C.

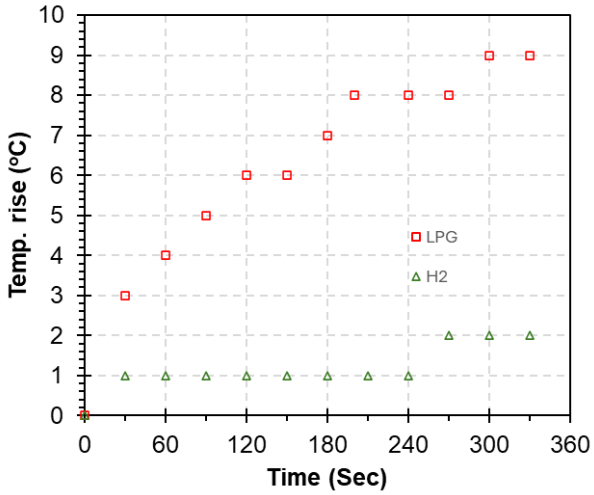


Fig. 11. Comparison of the effects of LPG and hydrogen flames on ambient temperature.

4. Discussion

4.1. System Performance and Operational Experience

The operational experience with the 1 kW solar-hydrogen cooking system over an extended period demonstrates the technical feasibility of decentralized hydrogen production and utilization for domestic cooking applications. The peak power output was limited to 1.1 kW by the 90 A MPPT current cap on the directly coupled electrolyser, reducing the daily solar-to-hydrogen conversion below what the 1.74 kWp array could otherwise deliver. Site-specific afternoon shading, which could not be avoided at this rooftop location, was largely responsible for the shortfall in daily yield relative to the array's rated capacity; in its absence, yield could potentially reach approximately 5 kWh/kWp. Because both the current cap and the shading loss are specific to this installation, the yield reported here should be read as a lower bound for a similarly sized system rather than an intrinsic ceiling on the technology.

The direct PV-electrolyser configuration also illustrates the importance of electrical matching in battery-free systems. During periods of high solar availability, the electrolyser operated at approximately 1 kW and produced hydrogen at rates approaching 3 L min-1. The electrolyser operating voltage decreased as its temperature increased, consistent with the temperature dependence of alkaline-electrolyser polarization behaviour. Dynamic operating conditions can influence alkaline electrolyser losses and performance, especially when the electrical input varies with renewable generation [35]. In the present system, the 90 A current cap prevented the PV array from fully utilizing the available power during high solar availability (10:00-14:20 h). Increasing this operating current limit, subject to the thermal and electrical limits of the electrolyser, could increase the hydrogen production without increasing the installed PV capacity.

The total H_2 production for the day is close to 1.3 m^3 during the characterization day, while the estimated water consumption was approximately 1.1 L. This corresponds to approximately 9.1 L of water per kilogram of hydrogen, which is close to the stoichiometric water requirement of approximately 9 kg per kg of H_2 for electrolysis. The observed value therefore does not indicate an unusually high direct water requirement for the demonstrated electrolysis process, although actual water demand can be higher when purification, cooling, and other balance-of-plant requirements are included. The hydrogen storage tank provided with the system ensures that any excess generation during peak hours can be stored and utilised during no sunshine or low sunshine periods. Because hydrogen can be consumed directly during periods of solar-driven production,

the storage requirement does not need to accommodate the entire daily cooking-energy demand. Considering that the morning cooking happens during sunlight hours, the storage of 63g (which is roughly half the total hydrogen generated) is sufficient for this stand-alone system, providing flexibility after solar-driven hydrogen production declines. This operating principle is a key difference between the demonstrated architecture and battery-buffered solar-electric cooking. Hydrogen is stored as hydrogen and used directly as a fuel rather than converting back to electricity before cooking.

4.2. Hydrogen burner performance relative to LPG

The hydrogen burner demonstrated cooking performance approaching that of the conventional LPG burner at the highest operating condition. At a hydrogen flow rate of 9.7 L min^{-1}, 1 L of water was heated from 30 °C to boiling in 6.2 min, compared with 5.0 min for the LPG burner at its high setting. The difference indicates that the hydrogen burner can provide a comparable heating rate under high-power operation, although it did not match the LPG burner exactly. At lower hydrogen flow rates, the time required to approach boiling increased substantially, demonstrating the importance of operating the burner within an appropriate power range for routine cooking.

The measured thermal efficiency of the hydrogen burner increased from 34.5% at 4.9 L min^{-1} to 46.0% at 9.7 L min^{-1}. The increase with flow rate is consistent with the greater useful heat input relative to the heat losses from the vessel at higher burner output. At lower heating rates, evaporative and convective losses become increasingly important, causing the water temperature to approach a thermal equilibrium below the boiling point. This behaviour was also observed for the LPG burner at its low setting, which reached only approximately 95 °C after 23 min. The results therefore indicate that the hydrogen burner can deliver practical cooking temperatures and heating rates when operated at sufficiently high flow rates.

The 46% thermal efficiency measured for the hydrogen burner should, however, be interpreted as a performance value for the present prototype rather than as an inherent efficiency advantage of hydrogen over LPG. The thermal efficiency of domestic LPG stoves in India is typically around 55-57%, while BIS-certified energy-efficient stoves have a minimum efficiency of 68% [34]. Experimental testing of a conventional domestic LPG stove has also reported efficiencies as low as 51% under adverse operating conditions [36]. The present results aim to demonstrate functional cooking performance and not greater efficiency. Further optimization of the burner and combustion system could improve the efficiency while retaining the advantages of the porous post-mixed burner configuration.

4.3. Thermal Comfort in the Cooking Environment

The temperature measurements indicate a potentially important difference between hydrogen and LPG cooking beyond fuel combustion and cooking performance. During the water-heating tests, the temperature near the cooking area increased by approximately 2 °C when the hydrogen burner was operated at 9.7 L min^{-1}, compared with an increase of approximately 9 °C for the LPG burner. Thus, under the tested conditions, the hydrogen burner was associated with an approximately 7 °C lower temperature rise in the monitored cooking area. This difference suggests that the hydrogen burner transferred less excess heat to the surrounding cooking environment, although the present measurements do not by themselves quantify human thermal comfort or physiological heat stress. The lower measured temperature rise may result from differences in flame characteristics, heat-release distribution, and the interaction between the burner and the cooking vessel. The burner used may alter the balance between useful heat transferred to the vessel and heat lost through radiation and convection compared with the LPG burner. To further characterize the contributions of these mechanisms would require measurements of flame temperature, radiative heat flux, convective losses, and spatial temperature fields. The present measurements should therefore be

interpreted as an assessment of the local thermal environment rather than a direct measurement of thermal comfort.

This distinction is important because indoor temperature is influenced by ventilation, outdoor conditions, building characteristics, humidity, and cooking activity, and elevated indoor temperatures can contribute to thermal discomfort and heat-related health risks (Head et al., 2018). The approximately 7 °C difference observed in the present controlled comparison therefore warrants further investigation as a potential thermal-comfort benefit of hydrogen cooking, particularly in hot climates. The findings support consideration of the cooking area thermal comfort as an additional performance metric for clean cooking technologies.

4.4. Implications for Sustainable Development

The global clean-cooking transition is currently constrained by two structural dependencies that this work addresses jointly. First, conventional clean fuels such as LPG rely on centralized, import-dependent supply chains that reproduce exactly the price volatility and rural–urban access gaps they are meant to resolve [2,37]. Second, the leading renewable alternative to fossil cooking fuels, battery-buffered solar electric cooking, substitutes this fuel-supply dependency for a dependency on electrochemical storage, carrying its own critical-mineral demand, degradation, and end-of-life burdens [38,39]. The novelty of the system reported here is that, by coupling the photovoltaic array directly to the electrolyser without a battery or power-conditioning stage, and by sustaining this architecture over months of real operation rather than a short laboratory or simulated demonstration, it decouples clean-cooking provision from both dependencies at once: the hydrogen produced is stored as a chemical fuel rather than electrochemically, and the fuel itself is generated on-site rather than delivered. This reframes the clean-cooking problem from one of substituting which fuel is delivered to a household, to one of eliminating delivery and battery-material dependence altogether, which is the structural barrier that most existing techno-economic assessments of clean cooking treat as fixed rather than addressable by system design. Realising this potential at scale will still depend on the cost, safety, and adoption evidence identified as future work above, but the present results establish, for the first time under sustained field conditions, that the underlying technical architecture is viable.

Beyond the measured performance of the system, the reductions in radiant heat and point-of-use emissions demonstrated here carry wider implications for health, gender equity, and climate goals.

In a country like India, where domestic cooking is largely done by women, a system of this kind could, if scaled and paired with adoption and affordability support, contribute to SDG 3 (good health and wellbeing), SDG 5 (gender equality) and SDG 7 (affordable and clean energy) [2,40]; demonstrating that contribution empirically would require the user-acceptance and time-use data this study did not collect. For context, all household cooking is estimated to account for approximately 1.69 GtCO2 globally, or approximately 3% of global emissions and about 56% of building-sector emissions; most of this total stems from solid biomass rather than LPG, so the mitigation potential of hydrogen-for-LPG substitution specifically is a smaller share that remains to be quantified, though any reduction achieved would still contribute to SDG 13 [40].

By reducing both pollution exposure and the heat stress borne by the person at the stove during cooking, with steady-state ambient temperatures lowered by approximately 7 °C relative to LPG, the proposed system offers a plausible route to easing daily cooking burdens and improving occupational thermal comfort; translating this into demonstrated gains for gender equality, migration or broader wellbeing would require dedicated social-science evaluation beyond the present engineering study [41].

Developing a replicable framework for deploying green hydrogen cooking systems in developing nations can serve as a vital climate resilience strategy. This approach will play a key role in achieving the UN's Clean Cooking Goal, which aims to eliminate cooking poverty and provide cleaner cooking solutions for all by 2030 and net-zero emissions by 2050 [2].

5. Conclusion

This study demonstrates the technical feasibility of a decentralized, battery-free solar-to-hydrogen system for household-scale clean cooking under real-world operating conditions. A 1.74 kWp photovoltaic array coupled to a 1 kW alkaline electrolyser produced approximately 1.3 m^3 of hydrogen during the representative clear-sky characterization day, corresponding to approximately 3.9 kWh of chemical energy on a lower-heating-value basis. The system has operated continuously since November 2024, demonstrating that hydrogen can serve as both the cooking fuel and the intermediate energy-storage medium without requiring battery storage.

The hydrogen burner achieved a thermal efficiency of up to 46% and, at 9.7 L min^{-1}, provided heating performance approaching that of the LPG burner tested under comparable conditions. Although the present burner does not yet demonstrate an efficiency advantage over high-efficiency LPG stoves, the results establish that hydrogen can provide practical cooking heat at household-relevant operating conditions. The field measurements also showed a substantially lower temperature rise in the cooking area with hydrogen than with LPG, with a difference of approximately 7 °C under the tested conditions. This finding indicates a potential thermal-environment benefit that warrants further investigation through direct measurements of thermal comfort and physiological heat stress.

The principal contribution of the study is therefore not simply the substitution of hydrogen for LPG, but the demonstration of an alternative household energy architecture in which renewable electricity is converted on-site into a storable chemical cooking fuel. By eliminating battery storage and reducing dependence on delivered cooking fuels, the demonstrated configuration offers a potential pathway toward greater household energy autonomy. However, broader deployment will require improvements in burner efficiency, optimization of PV–electrolyser matching, assessment of hydrogen-storage safety and durability, techno-economic and life-cycle evaluation, and field studies of user acceptance and long-term operation. The results provide an empirical foundation for evaluating decentralized solar-hydrogen systems as a potential complement to existing clean-cooking pathways.

References

[1] International Energy Agency. (2026). Energy crisis threatens world's most vulnerable as cooking fuel shortages grow. Retrieved from https://www.iea.org/commentaries/energy-crisis-threatens-worlds-most-vulnerable-as-cooking-fuel-shortages-grow?utm_source=chatgpt.com

[2] International Energy Agency, International Renewable Energy Agency, United Nations Statistics Division, World Bank, & World Health Organization. (2026). TRACKING SDG7 THE ENERGY PROGRESS REPORT 2026. Retrieved from https://trackingsdg7.esmap.org/sites/default/files/download-documents/SDG7-Report2026-0623-V4-4Web.pdf

[3] Wei, K., Lin, B. (2024). Spatial evolution of global household clean cooking energy transition: Convergent clubs and drivers, Applied Energy, 372, 123752.

[4] Roy, K. (2024). Transition to cooking with clean fuels in rural households of India: Studying the effect of policy and other factors. Energy for Sustainable Development, 80, 101456.

[5] Mishra, N. K., Biswas, P., & Patel, S. (2024). Future of clean energy for cooking in India: A comprehensive analysis of fuel alternatives. Energy for Sustainable Development, 81, 101500.

[6] Lombardi, F., Riva, F., Sacchi, M., & Colombo, E. (2019). Enabling combined access to electricity and clean cooking with PV-microgrids: New evidences from a high-resolution model of cooking loads. Energy for Sustainable Development, 49, 78–88.

[7] Araújo, A. C., Gomes, A., Rodrigues, P. M., & Silva, C. L. M. (2025). Advancing solar cooking: Challenges, innovations, and future directions. Energy Nexus, 19, 100521.

[8] Khatri, R., Goyal, R., Sharma, R. K. (2021). Advances in the developments of solar cooker for sustainable development: A comprehensive review. Renewable and Sustainable Energy Reviews, 145, 111166.

[9] Opoku, R., Baah, B., Sekyere, C.K.K., Adjei, E.A., Uba, F., Obeng, G.Y., Davis, F. (2022). Unlocking the potential of solar PV electric cooking in households in sub-Saharan Africa – The case of pressurized solar electric cooker (PSEC). Scientific African, 17, e01328. https://doi.org/10.1016/j.sciaf.2022.e01328

[10] Chaciga, J., Okello, D., Nyeinga, K., Nydal, O.J. (2025). Experimental analysis on a solar photovoltaic indoor cooker integrated with an energy storage system: A positive step towards clean cooking transition for Sub-Saharan Africa. Solar Compass, 13, 100109. https://doi.org/10.1016/j.solcom.2025.100109

[11] Nyeinga, K., Chaciga, J., Achire, T., Okello, D. (2025). Solar photovoltaic cooker: Technical analysis of a system suitable for institutional cooking. Energy 360, 4, 100047. https://doi.org/10.1016/j.energ.2025.100047

[12] Odoi-Yorke, F., Opoku, R., Davis, F., Obeng, G.Y. (2025). Advancing the solar cooking revolution: Insights into the evolving landscape of solar PV-based electric cooking. Solar Energy Advances, 5, 100091. https://doi.org/10.1016/j.seja.2025.100091

[13] Ramos-Galdo, S., Eras-Almeida, A.A., Mazorra Aguiar, J., Egido-Aguilera, M.A. (2025). Comprehensive approach for electricity and clean cooking access through solar photovoltaic mini grids: The Kobe refugee camp case study. Energy for Sustainable Development, 86, 101691. https://doi.org/10.1016/j.esd.2025.101691

[14] Selänniemi, A., Hellström, M., Björklund-Sänkiaho, M. (2024). Long-Duration Energy Storage—A Literature Review on the Link between Variable Renewable Energy Penetration and Market Creation. Energies, 17(15), 3779.

[15] Franco, A., & Giovannini, C. (2023). Recent and Future Advances in Water Electrolysis for Green Hydrogen Generation: Critical Analysis and Perspectives. Sustainability, 15(24), 16917.

[16] Mukelabai, M. D., Wijayantha, K. G. U., & Blanchard, R. E. (2022). Hydrogen for Cooking: A Review of Cooking Technologies, Renewable Hydrogen Systems and Techno-Economics. Sustainability, 14(24), 16964.

[17] Zhao, X., Ge, X., & Henry, C. (2025). Hydrogen as a clean cooking fuel: Technical and economic viability and barriers in developing countries. Energy for Sustainable Development, 89, 101852.

[18] Çolak, E., Yayla, R. (2026). Integrated green hydrogen strategic assessment framework for Türkiye: Sector prioritization, hydrogen valleys and policy roadmap. International Journal of Hydrogen Energy, 281, 157892. https://doi.org/10.1016/j.ijhydene.2026.157892

[19] Özçelep, Y., Bekdaş, G., Apak, S. (2021). Investigation of photovoltaic-hydrogen power system for a real house in Turkey: Hydrogen blending to natural gas effects on system design. International Journal of Hydrogen Energy, 46, 36678–36686. https://doi.org/10.1016/j.ijhydene.2021.08.186

[20] Gil Mena, A.J., Bouakkaz, A., Abelleira Pereira, J.M., Segovia Guerrero, L., Martín Rodríguez, M.L. (2024). Collective hydrogen stand-alone renewable energy systems for buildings in Spain. Towards the self-sufficiency. International Journal of Hydrogen Energy, 72, 1274–1286. https://doi.org/10.1016/j.ijhydene.2024.05.438

[21] Khan, S.A., Tao, Z., Agyekum, E.B., Fahad, S., Tahir, M., Salman, M. (2025). Sustainable rural electrification: Energy-economic feasibility analysis of autonomous hydrogen-based hybrid energy system. International Journal of Hydrogen Energy, 141, 460–473. https://doi.org/10.1016/j.ijhydene.2024.09.063

[22] Çiçek, A. (2025). Resilience-oriented energy operation of a country house sustained by fishing with renewable sources and hydrogen-based technologies. International Journal of Hydrogen Energy, 144, 947–963. https://doi.org/10.1016/j.ijhydene.2025.01.292

[23] González del Valle, A., García-Linares, P., & Martí, A. (2024). Optimizing hydrogen Production: A comparative study of direct and indirect coupling between photovoltaics and electrolyzer. Energy Conversion and Management, 315, 118751.

[24] Phan Van, L., Hieu Hoang, L., & Nguyen Duc, T. (2023). A comprehensive review of direct coupled photovoltaic-electrolyser system: Sizing techniques, operating strategies, research progress, current challenges, and future recommendations. International Journal of Hydrogen Energy, 48(65), 25231–25249.

[25] Mejía-Giraldo, D., Castillo-Ramírez, A., Velilla-Hernández, E. (2026). Techno-economic analysis of PV-based hydrogen production in Colombia: Policy perspectives on market competitiveness. International Journal of Hydrogen Energy, 242, 155472. https://doi.org/10.1016/j.ijhydene.2026.155472 [11] Bhandari R., Stadler I. (2011) Electrification using solar photovoltaic systems in Nepal. Applied Energy, 88, 458–65.

[26] Fumey, B., Stoller, S., Fricker, R., Weber, R., Dorer, V., Vogt, U.F. (2016). Development of a novel cooking stove based on catalytic hydrogen combustion. International Journal of Hydrogen Energy, 41, 7494–7499. https://doi.org/10.1016/j.ijhydene.2016.03.134

[27] Topriska, E.; Kolokotroni, M.; Dehouche, Z.; Wilson, E. Solar hydrogen system for cooking applications: Experimental and numerical study. Renew. Energy 2015, 83, 717–728.

[28] Topriska, E.; Kolokotroni, M.; Dehouche, Z.; Novieto, D.T.;Wilson, E.A. The potential to generate solar hydrogen for cooking applications: Case studies of Ghana, Jamaica and Indonesia. Renew. Energy 2016, 95, 495–509.

[29] Hutty, T., Hammond, J., Roberts, D., Barton, J., Wilson, J., Strickland, D., & Brown, S. (2024). Lead-acid battolysers for hydrogen cooking: A comparison with electric cooking for sub-Saharan Africa. Energy for Sustainable Development, 81, 101491.

[30] Odoi-Yorke, F., Abbey, A. A., Kaku, A., Afonaa-Mensah, S., Agyekum, E. B., Essuman, C. B., … Atepor, L. (2024). Evaluating the economic viability of decentralised solar PV-based green hydrogen for cooking in Ghana. Solar Compass, 11, 100078.

[31] Scott, M., Powells, G. (2020). Sensing hydrogen transitions in homes through social practices: Cooking, heating, and the decomposition of demand. International Journal of Hydrogen Energy, 45, 3870–3882. https://doi.org/10.1016/j.ijhydene.2019.12.025

[32] Gordon, J.A., Balta-Ozkan, N., Nabavi, S.A. (2024). Hopes and fears for a sustainable energy future: Enter the hydrogen acceptance matrix. International Journal of Hydrogen Energy, 60, 1170–1191. https://doi.org/10.1016/j.ijhydene.2024.02.247

[33] Gordon, J.A., Balta-Ozkan, N., Haq, A., Nabavi, S.A. (2024). Necessary and sufficient conditions for deploying hydrogen homes: A consumer-oriented perspective. International Journal of Hydrogen Energy, 69, 982–1021. https://doi.org/10.1016/j.ijhydene.2024.04.352

[34] Council on Energy, Environment and Water, Deutsche Gesellschaft für Internationale Zusammenarbeit, & NITI Aayog. (2019). Roadmap for Access to Clean Cooking Energy in India. NITI Aayog.

[35] Järvinen, L., Puranen, P., Ruuskanen, V., Kosonen, A., Kauranen, P., Ahola, J., & Chatzichristodoulou, C. (2024). Experimental study of alkaline water electrolyzer performance and frequency behavior under high frequency dynamic operation. International Journal of Hydrogen Energy, 67, 50–61.

[36] Bhatt, D. S., Mulla, I. A., & Dhamangaonkar, P. R. (2011). Design and Development of Burner Ring to Enhance Thermal Efficiency of Domestic LPG Stove and Assessment of its Performance. Int. Conf. on Recent Innovations in Technology, Kottayam, Kerala. 385-390

[37] Ministry of Health and Family Welfare. (2021). National Family Health Survey (NFHS-5) 2019-21: India Fact Sheet. New Delhi: Government of India. Retrieved from Government of India website: https://www.nfhsiips.in/nfhsuser/nfhs5.php

[38] Bielmann, M.; Vogt, U.F.; Zimmermann, M.; Züttel, A. Seasonal energy storage system based on hydrogen for self sufficient living. J. Power Sources 2011, 196, 4054–4060.

[39] Sun, S., Guan, T., Cheng, X., Zuo, P., Gao, Y., Du, C., & Yin, G. (2018). Accelerated aging and degradation mechanism of LiFePO4/graphite batteries cycled at high discharge rates. RSC Advances, 8(45), 25695–25703.

[40] World Health Organization. (2023). Achieving universal access and net-zero emissions by 2050. Retrieved 27 August 2026, from https://www.who.int/publications/m/item/achieving-universal-access-by-2030-and-net-zero-emissions-by-2050-a-global-roadmap-for-just-and-inclusive-clean-cooking-transition

[41] Head, K., Clarke, M., Bailey, M., Livinski, A., Ludolph, R., & Singh, A. (2018). Report of the systematic review on the effect of indoor heat on health. In WHO Housing and Health Guidelines. World Health Organization. Retrieved from https://www.ncbi.nlm.nih.gov/books/NBK535282/